Hindawi
Advances in Materials Science and Engineering
Volume 2019, Article ID 6235846, 10 pages
https://doi.org/10.1155/2019/6235846

Research Article

Study on the Process Optimization and Wear Resistance of Electron Beam Cladding WC-CoCr Coating on Inconel 617 Surface

Hailang Liu,[1,2] Yiping Huang,[1,2] Bo Wang,[1] and Xiaoyu Wang[1]

[1]*Guangxi Key Laboratory of Manufacturing Systems and Advanced Manufacturing Technology, Guilin University of Electronic Technology, Guilin 541004, China*
[2]*State Key Laboratory of Metal Material for Marine Equipment and Application, Anshan 114000, China*

Correspondence should be addressed to Yiping Huang; 1621758160@qq.com

Received 23 March 2019; Revised 16 July 2019; Accepted 22 July 2019; Published 19 August 2019

Academic Editor: Amelia Almeida

In order to enhance the high-temperature wear resistance of the nickel-base alloy, the electron beam is used to clad the WC-CoCr composite coating on the Inconel 617 surface. A six-factor and three-level orthogonal experiment is designed using Minitab software with scanning beam current, frequency, high voltage, beam spot diameter, offset sweep amplitude, and scanning speed as variables, and the variance and range of the test results are analyzed. The optimal cladding process parameters were determined according to the influence of various factors on the quality characteristics of the cladding layer. The wear behavior at 200°C, 600°C, and 1000°C and microstructure and phase composition of coating before and after electron beam treatment were tested. The results show that the ion exchange between the coating and the substrate is carried out after electron beam treatment. The WC, CoCr, (Fe, Ni)C6, Fe3W3C phase, and solid solution of α-Co were found in the cladding layer, and the microstructure of the coating is mainly dendrite and eutectic on CoCr substrate. The test of wear behavior at high temperature shows that the wear rate of the coating treated by electron beam at 200°C, 600°C, and 1000°C is 10.14 times, 6 times, and 2.29 times lower than that of the substrate, respectively. Moreover, the furrow and scratches of the cladding layer are less than those of the substrate at high temperature. The wear resistance of the coating was improved.

1. Introduction

Inconel 617 alloy is a nickel-base superalloy developed in early 1960s as an advanced alloy for high temperature, high strength, oxidation resistance, and corrosion resistance and used in gas turbine engines [1, 2]. In recent years, with the development of spaceflight industry in various countries, higher requirements on the wear resistance, corrosion resistance, and high-temperature oxidation resistance of 617 alloy have been put forward. It is urgent to improve the gas content, microstructure, and surface densification of the alloy to improve the properties and life of the alloy. Typically, the wear and corrosion of the alloy parts occur on the surface or surface layer. In order to overcome the deficiency, the method of preparing wear-resistant and corrosion-resistant coating on its surface is usually used to modify it. As one of the most widely used wear resistant coatings, WC is mainly used to resist severe wear (adhesive wear, abrasive wear, etc.) and combined with high-temperature corrosion and high-temperature oxidation performance [3, 4]. Moreover, the addition of elements such as Co, Cr, and Ni provides the necessary toughness and corrosion resistance for the WC-based coating [5–8]. At present, the main methods for preparing WC-based coatings are thermal spraying (e.g., plasma spraying, flame spraying, and arc spraying) [9–12]. Although thermal spraying has high spraying efficiency, the coating contains more pores and microcracks and is mechanically bonded on the substrate surface, which makes the coating fail prematurely. Moreover, the coating is easy to be oxidized and decomposed into W2C or W [13, 14]. The high melting point powder can be cladded on the surface of a low melting point substrate by

electron beam cladding to form a metallurgical cladding layer with metallurgical binding characteristics, and the surface hardness, wear resistance, and corrosion resistance of 617 alloy matrix can be significantly improved. Therefore, it has been favored by researchers in recent years.

However, for the electron beam cladding process, the cladding parameters are directly related to the quality of the cladding layer, which then directly affect the coating properties. The main parameters of electron beam cladding are scanning beam current, frequency, high voltage, beam spot diameter, offset sweep amplitude, and scanning speed [15, 16]. At present, the research on the optimization of electron beam cladding parameters is very rare due to the nonlinear relationship between the electron beam machining parameters and the coating quality which require a large number of experiments to verify it. Most researchers obtain empirical values through a large number of experiments. In order to reduce the number of experiments without reducing the feasibility of the tests, this paper proposes to select representative and typical test sites from a large number of test sites by using the principle of orthogonality and the knowledge of mathematical statistics. Then, the orthogonal table is used to arrange scientifically and reasonably, and the software is used to carry on the scientific orthogonal experiment design and the auxiliary data processing so as to improve the optimization efficiency. It provides an effective experimental method for optimizing the parameters of electron beam cladding.

2. Experiment

The size of Inconel 617 is $50 \times 30 \times 10$ mm, and the chemical composition is shown in Table 1. The matrix of Inconel 617 must be smoothed by using a sandpaper before cladding, and ultrasonic cleaning is carried out in acetone. The cladding material is WC-CoCr with a grain size of 50 μm~250 μm. Its alloy composition (mass fraction) is C, 10.15%; Co, 9.29%; and Cr, 3.50%, and W, margin.

The cladding experiment is carried out with SEB(j)6/60/40/30 electron beam machining integrated system. The purpose of the experiment is to optimize the parameters of electron beam processing so that the performance of the cladding layer can be improved. Optimization experiment is based on Minitab software to design different electron beam processing parameters for cladding of WC-CoCr on the surface of Inconel 617 substrate. The main process parameters that affect the quality of cladding layer when the vacuum level and machining distance were fixed are scanning beam, frequency, high voltage, beam spot diameter, and partial scanning amplitude. This experiment chooses $L_9(3^6)$ to design the orthogonal experiment. These six factors are recorded as A, B, C, D, E, and F, and each factor takes three levels. Table 2 is a table of factor levels.

The experimental design table is selected according to the factor level of Table 2, and the above factors were arranged in the order of 1~6 column in the test design table. The experiment scheme can be designed easily by using Minitab software. From "Statistics" ⟶ DOE ⟶ Taguchi ⟶ Create Taguchi design enter, select 6-factor number 3-level design and related parameters, obtain the output design table as shown in Table 3.

Table 1: Chemical composition of Inconel 617 alloy (wt.%).

Ni	Cr	Co	Mo	Al	C	Fe	Mn	Si	S	Ti	Cu
Balance	22	12.5	9	1.2	0.07	1.5	0.5	0.5	0.008	0.3	0.2

Electron beam scanning cladding experiments were carried out for each of the experimental design schemes in Table 3. The quality characteristics of the cladding layer (including surface quality, cladding phenomena, and microstructure of cladding cross section) were evaluated (10 points). The surface quality of the coating is mainly based on the accumulation of scum into a ball, the existence of cracks, and the number of pores in the coating. The phenomenon of cladding mainly determines either spatter or spatter degree, melting degree of powder, and width of melting pool. The microstructure mainly determines whether the metallurgical bonding is good or not, whether the microstructure is uniform or not, whether there are compositional segregation and porosity. According to these rules, depending on the degree, 0.5, 1, 1.5, and 2 are deducted, respectively, and the weight coefficient ratio of the three indexes is set to 0.4, 0.2, and 0.4 due to the influence degree of each index on the process. Therefore, the sum of each score multiplied by the weighting coefficient is the comprehensive score, which is also called the quality characteristic value. The results are shown in Table 4. Finally, through the analysis of range and variance, the optimal parameter combination is obtained [17].

The wear resistance of cladding samples was studied by using MPX-2000 vertical universal friction and wear tester. The test was carried out with a load of 20 N and a rotational speed of 200 r/min, and the test distance was 1000 meters (the radius of the sliding path was 5 mm). The wear weight loss is calculated using the equipment AR2130 electronic balance. The microhardness of the cross section between cladding and substrate is measured using HV-1000 microhardness meter. The section structure and element composition of WC-CoCr cladding layer are observed using Quanta 450 FEG field emission scanning electron microscope. The modified phase of the cladding is determined by D8ADVANCE X-ray diffractometer, and the ray source is Cu-Kα, and the data are collected in the range of 2θ to 20°~100°.

3. Experimental Results and Analysis

3.1. Range Analysis of Orthogonal Experiment Results. The results of the range analysis of the quality characteristics of the cladding layer are detailed in Table 5. (1) The relation of the size of each factor in Table 5 is $0.759(A) > 0.537(F) > 0.407(D) > 0.167(C) > 0.131(E) > 0.130(B)$. The primary and secondary orders that can be deduced to affect the quality characteristic y are scanning beam current, scanning speed, beam spot diameter, high voltage, skew sweep amplitude, and frequency. (2) Based on the calculation and analysis of the test results in Table 4, we compare the value of each factor Iy, IIy, and IIIy with each other and take the level

Table 2: Orthogonal experimental factor level.

Level	Factor					
	A Scanning beam (mA)	*B* Frequency (Hz)	*C* High voltage (kV)	*D* Beam spot diameter (mm)	*E* Partial scanning amplitude (%)	*F* Scanning speed (mm/min)
1	80	500	50	8	2	800
2	83	550	55	9	4	1000
3	85	600	60	10	6	1200

Table 3: Cladding orthogonal experiment of WC-CoCr.

Number	Factor					
	A (mA)	*B* (Hz)	*C* (kV)	*D* (mm)	*E* (%)	*F* (mm/min)
1	80	500	50	8	2	800
2	80	500	50	8	4	1000
3	80	500	50	8	6	1200
4	80	550	55	9	2	800
5	80	550	55	9	4	1000
6	80	550	55	9	6	1200
7	80	600	60	10	2	800
8	80	600	60	10	4	1000
9	80	600	60	10	6	1200
10	83	500	55	10	2	1000
11	83	500	55	10	4	1200
12	83	500	55	10	6	800
13	83	550	60	8	2	1000
14	83	550	60	8	4	1200
15	83	550	60	8	6	800
16	83	600	50	9	2	1000
17	83	600	50	9	4	1200
18	83	600	50	9	6	800
19	85	500	60	9	2	1200
20	85	500	60	9	4	800
21	85	500	60	9	6	1000
22	85	550	50	10	2	1200
23	85	550	50	10	4	800
24	85	550	50	10	6	1000
25	85	600	55	8	2	1200
26	85	600	55	8	4	800
27	85	600	55	8	6	1000

corresponding to the maximum value of the three values as the optimum level of the factor to y, and then the optimum level of each factor is as follows: scanning beam current A (85 mA), frequency B (600 Hz), high voltage C (60 kV), beam spot diameter D (8 mm), offset scan value E (4%), scanning speed F (1000 mm/min). From Figure 1, it can be seen that the curve of scanning current, scanning velocity, and beam spot diameter fluctuates greatly, which has a great influence on the quality characteristics of the cladding layer. And at the experimental level, the larger the scanning current, the larger the mass characteristic value.

3.2. Analysis of Variance of Orthogonal Experiment Results. The range analysis does not distinguish the data fluctuation caused by the test error from the data fluctuation caused by the change of the test conditions nor does it examine whether the effect of various factors on the test results (indicators) is significant. So we do not know how accurate the analysis is. To make up the shortcomings of the above intuitive analysis, the following uses the method of variance analysis to further estimate the magnitude of the error and accurately estimate the importance of each factor affecting the test results. The variance analysis results of the cladding quality characteristics are shown in Table 6.

S_j is calculated using the following formula:

$$S_j = K_j\left(\mathrm{I}_j - \overline{y}\right)^2 + K_j\left(\mathrm{II}_j + \overline{y}\right)^2 + K_j\left(\mathrm{III}_j - \overline{y}\right)^2, \quad (1)$$

where I_j, II_j, and III_j are the average of the test indicators of the j levels, $\overline{y}$ is the average of test indicators, and K_j is the number of occurrences at the same level. It can be seen that the information provided by the data can be fully utilized when the square error of deviation is represented, but the error will also increase with the increase in the test data. It can be transformed into

$$\begin{aligned} S_j &= S \cdot f_j, \\ \mathrm{SS} &= \mathrm{Ms} \cdot f_j, \\ S &= \sqrt{\mathrm{Ms}} \Longrightarrow S_j = \mathrm{SS} \cdot \mathrm{Ms}. \end{aligned} \quad (2)$$

Thus, the mean square Ms can be obtained. The influence trend of each factor on cladding characteristics can be compared from the numerical analysis of Ms. And by comparing the magnitude of Ms value corresponding to each factor, the fluctuation results are in agreement with the range analysis. The P value represents the probability of the hypothesis that the average value is equal in the group, and the smaller it is, the more significant the effect of the factors on the test index is. When PA < 0.01, the effect of A (scanning beam current) on the mass characteristic value is very significant and PF < 0.05 and PD < 0.05 indicates that F (scanning speed) and D (beam spot diameter) also have a significant effect on the quality characteristic value. The effect of beam spot diameter is less than that of the first two factors. The analysis of the F value of each factor deviates greatly from 1, which shows that its influence is very great. Thus FB, FC, and FE in the vicinity of 1 indicates that its influence is weak.

Through the above analysis, taking the quality characteristic value of cladding experiment as the evaluation index, it is concluded that the influence of factors on the test index is in the order of scanning beam current > scanning speed > beam spot diameter > high voltage > deviation sweep amplitude > frequency. The optimized level is scanning current 85 mA, high voltage 60 kV, frequency 600 Hz, beam spot diameter 8 mm, offset scan amplitude 4%, and scanning speed 1000 mm/min. Among the factors of "scanning

Table 4: WC-CoCr orthogonal experiment results.

No.	Factor						Quality characteristic			
							Number of scores per item			
	A (mA)	B (Hz)	C (kV)	D (mA)	E (%)	F (mm/min)	Surface quality	Cladding phenomenon	Microstructure	Total score
1	80	500	50	8	2	800	8.0	7.0	7.0	7.4
2	80	500	50	8	4	1000	9.0	8.5	8.5	8.7
3	80	500	50	8	6	1200	8.5	9.0	8.5	8.6
4	80	550	55	9	2	800	8.0	7.5	8.0	7.9
5	80	550	55	9	4	1000	8.0	8.0	8.5	8.2
6	80	550	55	9	6	1200	7.5	7.0	7.0	7.2
7	80	600	60	10	2	800	7.0	6.0	7.0	6.8
8	80	600	60	10	4	1000	8.5	7.0	7.5	7.8
9	80	600	60	10	6	1200	9.0	7.5	8.5	8.5
10	83	500	55	10	2	1000	9.0	8.0	8.0	8.4
11	83	500	55	10	4	1200	8.5	7.5	9.0	8.5
12	83	500	55	10	6	800	8.5	7.0	7.5	7.8
13	83	550	60	8	2	1000	9.0	8.5	8.5	8.7
14	83	550	60	8	4	1200	8.0	8.0	8.5	8.2
15	83	550	60	8	6	800	8.5	7.5	7.5	7.9
16	83	600	50	9	2	1000	9.5	8.0	8.5	8.8
17	83	600	50	9	4	1200	7.5	7.5	7.5	7.5
18	83	600	50	9	6	800	8.5	8.0	7.5	8.0
19	85	500	60	9	2	1200	9.0	8.5	8.5	8.7
20	85	500	60	9	4	800	9.5	8.0	9.0	9.0
21	85	500	60	9	6	1000	7.5	8.0	8.0	7.8
22	85	550	50	10	2	1200	8.5	7.5	9.5	8.7
23	85	550	50	10	4	800	8.5	7.0	8.0	8.0
24	85	550	50	10	6	1000	9.5	9.0	8.5	9.0
25	85	600	55	8	2	1200	9.0	8.5	8.0	8.5
26	85	600	55	8	4	800	9.0	9.5	9.0	9.1
27	85	600	55	8	6	1000	9.5	9.0	8.5	9.0

Table 5: Calculation table of range analysis test results.

Number	A	B	C	D	E	F
Iy	7.833	8.259	8.241	8.444	8.130	7.907
IIy	8.130	8.130	8.241	8.074	8.259	8.444
IIIy	8.593	8.167	8.074	8.037	8.168	8.204
Ry	0.759	0.130	0.167	0.407	0.131	0.537

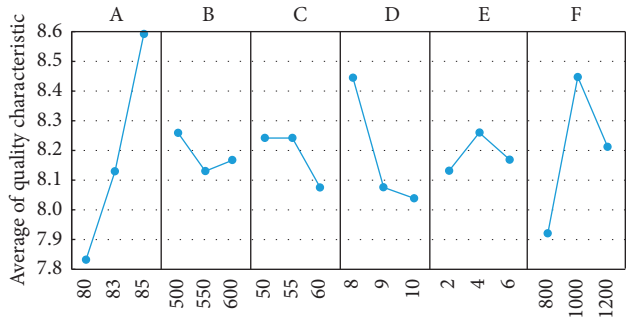

Figure 1: Trend chart of correlation between factors and quality characteristic values.

beam," "scanning velocity," and "beam spot diameter," $P < 0.05$, which means that these factors have a significant effect on the test results, while other factors $P > 0.05$, which means that they have no significant influence on the test results (as shown in Table 7).

3.3. Effect of Main Parameters on Cladding Layer. According to the results of orthogonal experiments, the main parameters that have a significant effect on the coating are electron beam current and electron beam scanning speed. And the electron beam spot diameter also has a certain effect on the coating, which is smaller than that of the first two. Figures 2–5 show the thickness of the coating layer and the microstructure of the coating section with different electron beam current and scanning speeds, respectively.

The effect of electron beam current on the cladding of WC-CoCr coating is as follows: with the increase of beam current, the quality of the coating becomes better. And the thickness of the coating increases and becomes uniform (as shown in Figures 2 and 3). The reason is that the beam current is too small, the output power of the electron beam is not enough, the surface temperature of the specimen rises slowly, the time of reaching the melting point of WC-CoCr is too long, and the cooling rate is slower. As a result, G/R becomes larger (G is the temperature gradient, and R is the solidification rate), which results in coarse dendritic structure. As the beam current increases, the G/R decreases and the component undercooling gradually increases so that the dendritic structure of the cladding layer is refined and uniform. When the output power of the electron beam is large enough to melt the WC-CoCr coating instantly, the optimum cladding effect can be achieved, the surface melting pool becomes deeper, the workpiece accumulates

Table 6: Analysis results of quality characteristics of the WC-CoCr cladding layer.

Source	Free degree f_j	Sum of squares S_j	Sum of squares of deviations SS	Mean square MS	F	P
A	2	3.18655	2.52519	1.26259	36.926	0.005
B	2	0.00288	0.07630	0.03815	1.1473	0.895
C	2	0.00672	0.11630	0.05815	1.7912	0.845
D	2	0.17316	0.58963	0.29481	8.6975	0.044
E	2	0.00482	0.09852	0.04926	1.4823	0.867
F	2	0.63675	1.12963	0.56481	16.581	0.0227
Error	14	0.01641	0.47918	0.03422	—	—

Table 7: Test results.

	Visual analysis		Variance analysis		
	Primary and secondary order	Optimal parameter	Highly significant	Notable	Quiet
Quality characteristic	*A F D C E B*	*A3B3C3D1E2F2*	*A*	*F D*	*C E B*

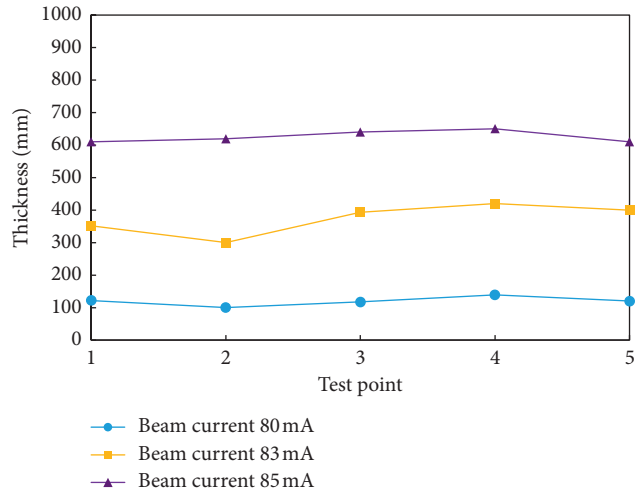

Figure 2: Thickness of the coating with different beam current.

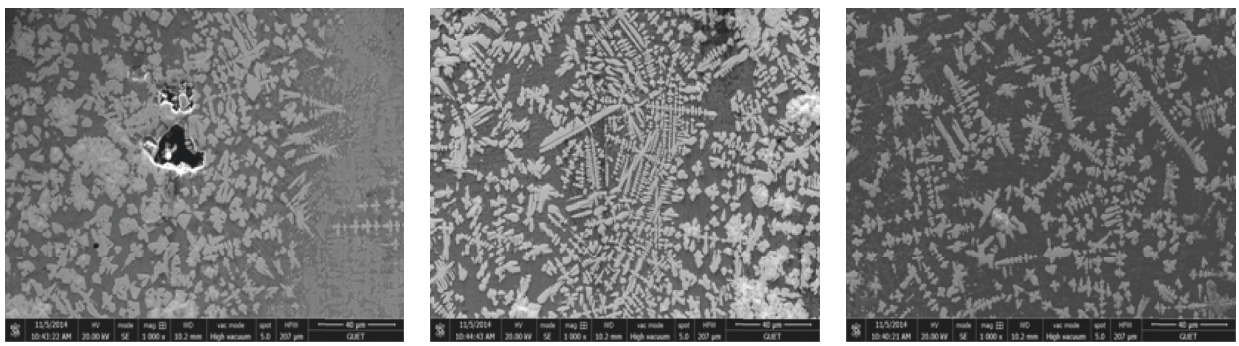

(a) (b) (c)

Figure 3: Microstructure of coating cross section with different beam current: (a) 80 mA, (b) 83 mA, and (c) 85 mA.

more heat, the temperature gradient of the specimen increases, and the cooling rate becomes slower. Dendritic structure cannot achieve the effect of refinement. The effect of scanning velocity is that the quality of cladding surface becomes better and the thickness of cladding decreases with the increase in velocity (as shown in Figures 4 and 5). The speed of scanning speed determines how much energy is input by electron beam to the melting pool per unit area of the sample surface. Within a certain range of parameters, the faster the scanning speed, the less the pool energy input, the smaller the size of the pool, and the faster the solidification, so the better the surface quality of the cladding layer. When the scanning speed is relatively slow, the thickness and width of the melting pool increase when the coating melts

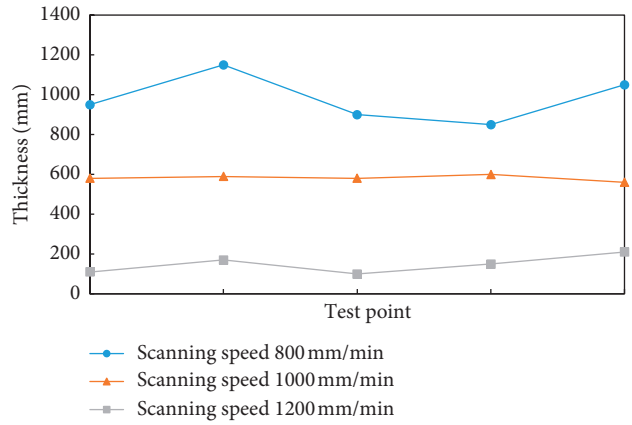

Figure 4: Thickness of the coating with different scanning speeds.

Figure 5: Microstructure of coating cross section with different scanning speeds: (a) 800 mm/min, (b) 1000 mm/min, and (c) 1200 mm/min.

thoroughly, but the electron beam spot stays on the surface of the specimen for a long time, and some WC-CoCr coating splashes occur, which results in the decrease in the thickness of the cladding layer after solidification. At the same time, because of the small speed, the cooling of the molten pool slowed down and gradually accumulated in the middle, forming the phenomenon of the central uplift. However, if the scanning speed is too fast, the input of energy on the surface of the specimen will be insufficient, resulting in poor formation of the cladding layer, resulting in coarse dendrite structure and defects in the inner surface such as the unmelted rigid WC-CoCr coating particles and pores. The effect of beam spot diameter is less than that of the first two factors, which is directly related to the spot area of electron beam and thus affects the magnitude of energy density. With the decrease of beam spot diameter, the energy density of electron beam increases, and the quality of cladding gradually becomes better. However, if the diameter of the electron beam spot is too small, the energy distribution is uneven and the coating effect is poor because of the excessive concentration of energy.

3.4. Element Composition and Phase Composition of Cladding Layer. The microstructure of the electron beam cladding WC-CoCr alloy layer after optimizing the parameters is compact, and the cladding layer mainly consists of dendritic crystal and a plurality of eutectic compositions. The microstructure and substrate of the cladding layer were analyzed by EDS. The location of the test area is shown in Figure 6. The content of the elements of the cladding was changed compared with the original coating powder. And new elements such as Ni, Fe, Mn, and Mo have been used. These indicate that the elements between the coating and the substrate are interdiffused during cladding. However, there are no elements such as Si and Ti in the cladding, which may be due to the low concentration of the elements themselves in the matrix, or they may not be distributed in the test area. Table 8 shows the percentage of test area elements. In addition, due to the characteristics of high-speed heat and rapid cooling in the process of electron beam cladding, there are no cracks, pores, inclusions, and segregation defects in the cladding layer. There is no gap between the substrate and the cladding layer, and a good metallurgical bonding is formed between them. The bonding strength between the coating and the substrate is one of the important indexes to meet the mechanical, physical, and chemical properties of the coating.

Figure 7 shows the XRD analysis of the electron beam cladding layer. The coating mainly consists of WC (#51-0939) and CoCr (#09-0052) phase and also contains (Fe, Ni) C_6 (#25-0405), Fe_3W_3C (#78-1990), α-Co (#05-0727) phases, and α-Co solid solution. The high-temperature environment of electron beam irradiation promotes the formation of complex carbides, among which the ternary carbides

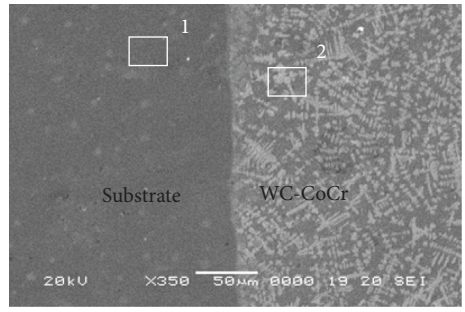

Figure 6: SEM diagram of cross section of WC-CoCr coating of electron beam cladding; 1: area 1; 2: area 2.

Table 8: Element percentage (wt.%).

Area	Ni	Cr	Co	Mo	W	C	Fe	Mn	Si	Al	Ti	Cu
1	46.94	5.4	10.3	7.68	16.7	9.2	1.3	0.3	0.42	0.86	0.52	0.38
2	6.88	2.8	13.2	1.2	66.8	8.52	0.3	0.1	—	0.2	—	—

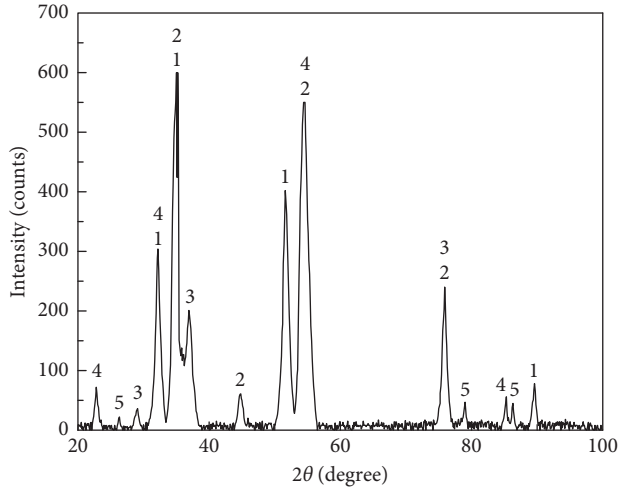

1. WC
2. CoCr
3. α-Co
4. Fe_3W_3C
5. (Fe, Ni) C_6

Figure 7: XRD diffraction pattern of the WC-CoCr cladding layer.

Fe_3W_3C have higher hardness, and WC are the main phase structure to improve the hardness and wear resistance of the cladding layer. The high hard phase coating contains more WC, which plays an important role in improving the wear resistance of the surface layer. However, an excessive WC content will result in poor bonding between the two phases of cermet, and there is not enough metal phase between the hard phase to play the role of bonding. In the process of friction, it is easy to fall off and become new debris, which accelerates the wear process of abrasive particles. The CoCr phase has better toughness and corrosion resistance than the hard WC phase, and it is distributed in the whole cladding as a soft substrate. In the process of electron beam cladding, a large degree of undercooling will be produced, together with the nonequilibrium and rapid cooling characteristics during solidification, which makes it easy for the rich W phase to form a specific crystal branch distributed in the CoCr substrate, thus realizing a certain strong and tough coordination. α-Co is a solid solution phase with face-centered cubic crystal structure, which precipitates preferentially as primary phase during solidification, which enhances the toughness of hard phase. In addition, the diffraction peak of the cladding layer is wider, which further proves that the WC-CoCr coating obtained by the cladding parameters is smaller in grain size.

3.5. Wear Rate and Friction Coefficient of Cladding at High Temperature. The friction coefficient is mainly related to the roughness of the surface and has nothing to do with the size of the contact surface. It can be seen from Figure 8 that the friction coefficient of the cladding layer is lower than that of the substrate at any temperature after electron beam scanning. It shows that the cladding layer is more wear-resistant

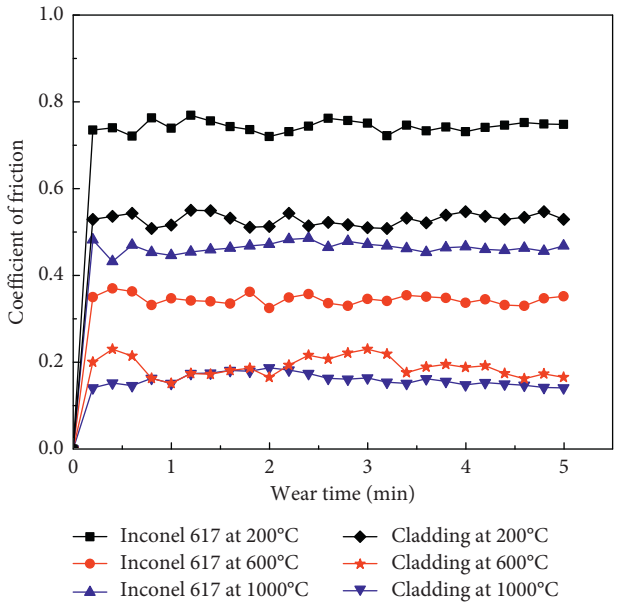

Figure 8: The curve of the friction coefficient varies with time of Inconel 617 alloy matrix and cladding at 200°C, 600°C, and 1000°C.

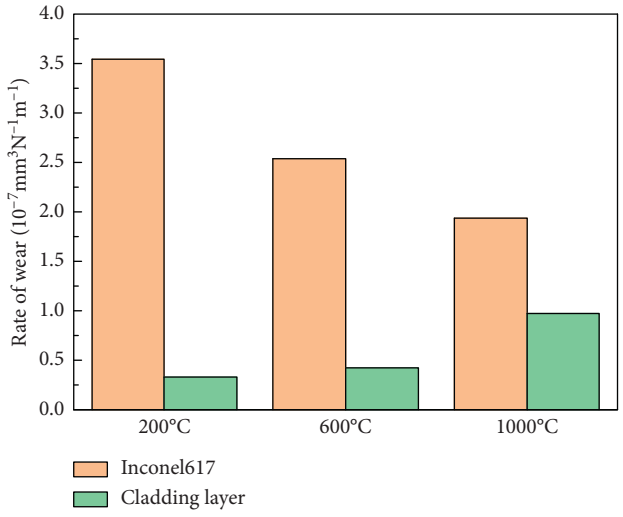

Figure 9: Wear rate of Inconel 617 alloy substrate and cladding at different temperatures.

than Inconel 617 alloy, which fully shows the effect of the hard phase of the cladding layer.

The friction coefficient of the cladding layer and Inconel 617 alloy decreases with the increase in temperature. This is the result of a combination of two factors: (1) With the increase in temperature, the surface of the cladding layer and Inconel 617 alloy softens, and the friction coefficient increases. (2) In the high-temperature environment, the two materials react with oxygen in the atmosphere and form an oxide film on the surface of the material, which can lubricate the friction between the material surface and SiC, and the friction coefficient becomes smaller. The combined effect of these two factors shows that the softening phenomenon is not obvious at the temperature of 200°C to 600°C, the lubricating effect of oxide film is stronger, and the friction coefficient of Inconel 617 alloy decreases faster than that of cladding layer. Between 600°C and 1000°C, the surface softening of the material is serious, and the friction coefficient decreases steadily.

Figure 9 shows a comparison of wear rates between Inconel 617 alloy substrates and cladding layers at different temperatures. It can be seen from the diagram that the wear rate of the cladding layer is lower than that of Inconel 617 alloy matrix at 200°C, 600°C, and 1000°C, respectively. Wear resistance is usually expressed in terms of the amount of wear or the reciprocal of the wear rate, that is, abrasive resistance = dL/dV or dt/dV. So the wear resistance of the cladding layer at 200°C is 10.14 times as high as that of Inconel 617 alloy. It is 6 times and 2.29 times higher than that of Inconel 617 alloy substrate at 600°C and 1000°C, respectively. With the increase in temperature, the wear rate of the substrate decreases gradually, while the wear rate of the cladding layer increases gradually, which is due to the oxidation of Inconel 617 alloy at high temperature and the lubricating effect of the oxide film formed. During friction with SiC at high temperature, the hard phase of the cladding layer is easy to fall off and becomes abrasive, which intensifies the wear of the cladding surface, so the wear rate of the cladding layer increases with the increase in temperature.

Figure 10 shows the wear morphology of Inconel 617 alloy substrate and cladding at 200°C, 600°C, and 1000°C. At 200°C, deep ploughing and scratching appeared on the wear surface of the matrix, and the wear mechanism was abrasive wear (Figure 10(a)). However, the surface of the WC-CoCr cladding layer is only slightly scratched at this temperature (Figure 10(d)). At 600°C, there were more scratches, uneven surface, and obvious ploughing on the surface of Inconel 617 alloy, but the wear morphology was better than that at 200°C (Figure 10(b)). The reason is that the surface of the matrix begins to oxidize at 600°C, and the following chemical reactions occur:

$$Al^{3+} + O^{2-} \longrightarrow Al_2O_3 \quad (3)$$

$$Cr^{3+} + O^{2+} \longrightarrow Cr_2O_3 \quad (4)$$

The formed Al_2O_3 and Cr_2O_3 oxide films cover the substrate surface and play a certain role in lubrication. Thus, the wear on the surface of the matrix is reduced. However, the high-temperature oxidation resistance of Inconel 617 matrix is better. At 200°C, the oxidation resistance grade of Inconel 617 matrix is complete oxidation resistance. The wear scratches of WC-CoCr coatings at 600°C increased compared with those at 200°C (Figure 10(e)). One reason is that in high-temperature friction, the damage caused by the peeling of hard particles of the coating is greater than the lubricating effect of the formation of oxide film. Moreover, the hard phase of WC is easily decomposed into W or W_2C at high temperature, which reduces the wear resistance of the cladding layer. There are fewer scratches in Inconel 617 matrix at 1000°C because of the lubricating effect of a large number of oxide films (Figure 10(c)). At the same time, the matrix has the lowest friction coefficient and wear rate at

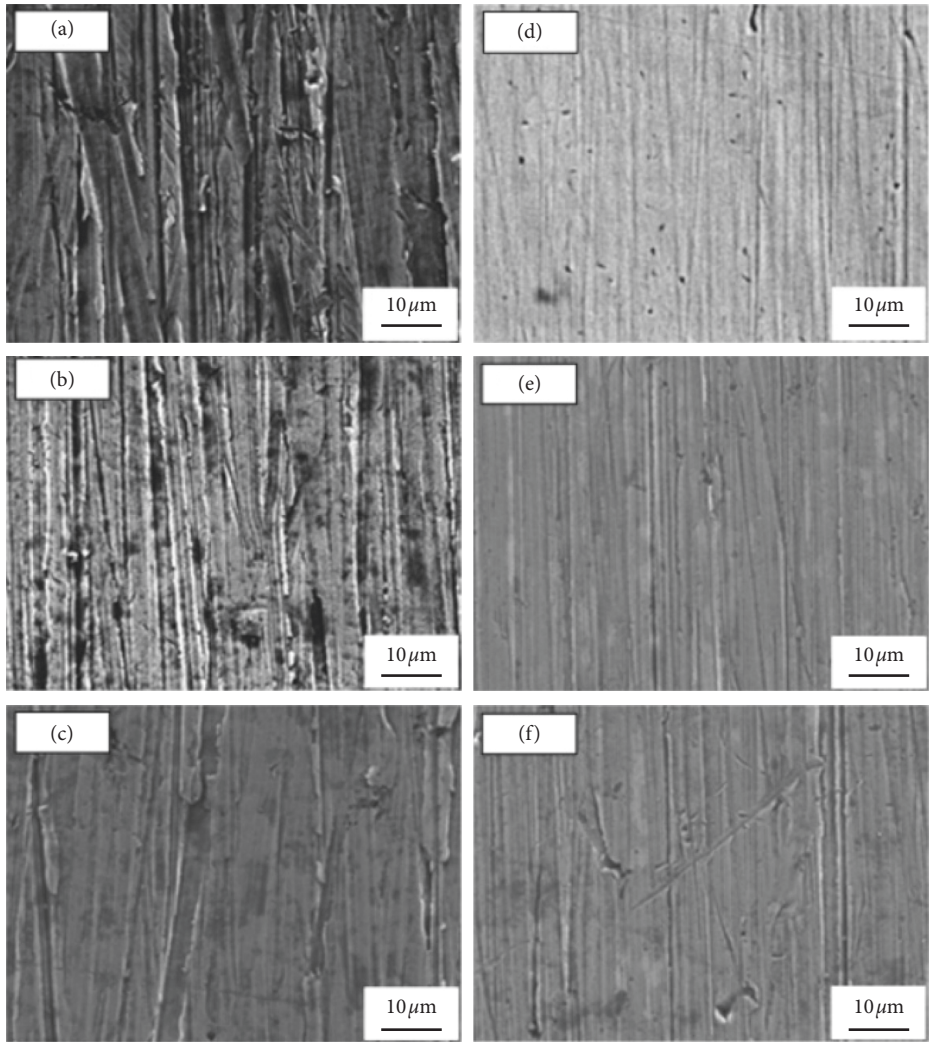

Figure 10: Wear morphology of Inconel 617 alloy substrate and cladding at different temperatures: (a) 200°C, (b) 600°C, and (c) 1000°C. Cladding at (d) 200°C, (e) 600°C, and (f) 1000°C.

1000°C compared with other temperature. The WC-CoCr cladding layer at 1000°C has a slight ploughing and crater due to the decomposition and exfoliation of hard phase at high temperature (Figure 10(f)).

4. Conclusion

(1) The optimum cladding parameters of Inconel 617 surface electron beam cladding WC-CoCr are obtained by orthogonal experiment: scanning beam current 85 mA, frequency 60 Hz, high voltage 60 kV, beam spot diameter 8 mm, scanning amplitude 4%, and scanning speed 1000 mm/min. The effects of these parameters on the quality characteristics of the cladding layer are as follows: scanning beam current, scanning speed, beam spot diameter, high voltage, skew sweep amplitude, and frequency, and scanning beam current is very significant, scanning speed and beam spot diameter are significant, and the rest has no significant effect.

(2) Compared with the original sprayed powder, new elements such as Ni, Fe, Mn, and Mo appeared in the cladding layer, and the content of the original elements changed. The metallurgical bonding was realized between the coating and the substrate. The rapid heat quenching effect of electron beam treatment results in the formation of new phases such as WC, CoCr, (Fe, Ni)C6, Fe3W3C, and Co in the cladding layer, in which intermetallic compounds and carbides are distributed in the CoCr matrix, which plays a strengthening role.

(3) The wear resistance of the cladding layer was 10.14 times of that of the substrate at 200°C. When the temperature exceeds 600°C, the surface softening phenomenon increases, the lubricant film is strengthened, the friction coefficient decreases, and the friction coefficient of the matrix decreases faster than that of the cladding layer. With the increase in temperature, the wear rate of the cladding layer decreases due to the easy oxidation of the substrate

and the wear rate of the cladding layer increases by 2.29 times as much as that of the substrate at 1000°C. At the test temperature, the friction coefficient and wear rate of the cladding layer are lower than that of the substrate, and the wear resistance of the cladding layer is improved.

Data Availability

The data used to support the findings of this study are available from the corresponding author upon request.

Conflicts of Interest

The authors declare that they have no conflicts of interest.

Acknowledgments

This work was financially supported by the Foundation Project of the Guangxi Key Laboratory of Manufacturing System and Advanced Manufacturing Technology (17-259-05-0068) and also supported by the Foundation Project of the State Key Laboratory of Metal Material for Marine Equipment and Application (SKLMEA-K201801).

References

[1] G. H. Bai, R. Hu, J. S. Jin et al., "Secondary M23C6 precipitation behavior in Ni-Cr-W based superalloy," *Rare Metal Materials and Engineering*, vol. 40, no. 10, pp. 1737–1741, 2011.

[2] G. A. El-Awadi, S. Abdel-Samad, and E. S. Elshazly, "Hot corrosion behavior of Ni based Inconel 617 and Inconel 738 superalloys," *Applied Surface Science*, vol. 378, pp. 224–230, 2016.

[3] C. T. Kunioshi, O. V. Correa, and L. V. Ramanathan, "High temperature oxidation and erosion-oxidation behaviour of HVOF sprayed Ni-20Cr, WC-20Cr-7Ni and Cr3C2-Ni-20Cr coatings," *Surface Engineering*, vol. 22, no. 2, pp. 121–127, 2006.

[4] C. Zheng, Y. Liu, J. Qin, C. Chen, and R. Ji, "Wear behavior of HVOF sprayed WC coating under water-in-oil fracturing fluid condition," *Tribology International*, vol. 115, pp. 28–34, 2017.

[5] A. Karimi, C. Verdon, and G. Barbezat, "Microstructure and hydroabrasive wear behaviour of high velocity oxy-fuel thermally sprayed WC-Co(Cr) coatings," *Surface and Coatings Technology*, vol. 57, no. 1, pp. 81–89, 1993.

[6] O. Culha, M. Toparli, E. Celik, T. Aksoy, and H. S. Soykan, "Indentation size effect on mechanical properties of HVOF sprayed WC based cermet coatings for a roller cylinder," *Surface and Coatings Technology*, vol. 203, no. 14, pp. 2052–2057, 2009.

[7] Z. Geng, S. Hou, G. Shi, D. Duan, and S. Li, "Tribological behaviour at various temperatures of WC-Co coatings prepared using different thermal spraying techniques," *Tribology International*, vol. 104, pp. 36–44, 2016.

[8] H. Chen, C. Xu, Q. Zhou, I. M. Hutchings, P. H. Shipway, and J. Liu, "Micro-scale abrasive wear behaviour of HVOF sprayed and laser-remelted conventional and nanostructured WC-Co coatings," *Wear*, vol. 258, no. 1–4, pp. 333–338, 2005.

[9] S. Hong, Y. Wu, B. Wang, J. Zhang, Y. Zheng, and L. Qiao, "The effect of temperature on the dry sliding wear behavior of HVOF sprayed nanostructured WC-CoCr coatings," *Ceramics International*, vol. 43, no. 1, pp. 458–462, 2017.

[10] L. Zhao, M. Maurer, F. Fischer, and E. Lugscheider, "Study of HVOF spraying of WC-CoCr using on-line particle monitoring," *Surface and Coatings Technology*, vol. 185, no. 2-3, pp. 160–165, 2004.

[11] X. Y. Cui, C. B. Wang, J. J. Kang, W. Yue, Z. Q. Fu, and L. N. Zhu, "Influence of the corrosion of saturated saltwater drilling fluid on the tribological behavior of HVOF WC-10Co4Cr coatings," *Engineering Failure Analysis*, vol. 71, pp. 195–203, 2017.

[12] W. Zhou, K. Zhou, Y. Li, C. Deng, and K. Zeng, "High temperature wear performance of HVOF-sprayed Cr3C2-WC-NiCoCrMo and Cr3C2-NiCr hardmetal coatings," *Applied Surface Science*, vol. 416, pp. 33–44, 2017.

[13] Q. Wang, Z. H. Chen, and Z. X. Ding, "Performance of abrasive wear of WC-12Co coatings sprayed by HVOF," *Tribology International*, vol. 42, no. 7, pp. 1046–1051, 2009.

[14] M. Jafari, M. H. Enayati, M. Salehi, S. M. Nahvi, and C. G. Park, "Microstructural and mechanical characterizations of a novel HVOF-sprayed WC-Co coating deposited from electroless Ni-P coated WC-12Co powders," *Materials Science and Engineering: A*, vol. 578, no. 8, pp. 46–53, 2013.

[15] I. A. Bataev, D. O. Mul, A. A. Bataev et al., "Structure and tribological properties of steel after non-vacuum electron beam cladding of Ti, Mo and graphite powders," *Materials Characterization*, vol. 112, pp. 60–67, 2016.

[16] S. F. Gnyusov and S. Y. Tarasov, "The microstructural aspects of abrasive wear resistance in composite electron beam clad coatings," *Applied Surface Science*, vol. 293, no. 3, pp. 318–325, 2014.

[17] D. C. Montgomery, "Design and analysis of experiments," *Technometrics*, vol. 48, no. 2, p. 245, 2001.